Excitation-Wavelength-Dependent, Ultrafast Photoinduced Electron Transfer in Bisferrocene/BF2-Chelated-Azadipyrromethene/Fullerene Tetrads

ARTICLE *in* CHEMISTRY - A EUROPEAN JOURNAL · MAY 2013

Impact Factor: 5.73 · DOI: 10.1002/chem.201204317 · Source: PubMed

7 AUTHORS, INCLUDING:

Mohamed E El-Khouly
Kafrelsheikh University
129 PUBLICATIONS **3,162** CITATIONS
SEE PROFILE

Kei Ohkubo
Osaka University
395 PUBLICATIONS **9,560** CITATIONS
SEE PROFILE

Volodymyr V Nesterov
New Mexico Highlands University
318 PUBLICATIONS **1,384** CITATIONS
SEE PROFILE

Melvin E Zandler
Wichita State University
107 PUBLICATIONS **3,343** CITATIONS
SEE PROFILE

CHEMISTRY
A EUROPEAN JOURNAL

FULL PAPER

DOI: 10.1002/chem.201204317

Excitation-Wavelength-Dependent, Ultrafast Photoinduced Electron Transfer in Bisferrocene/BF_2-Chelated-Azadipyrromethene/Fullerene Tetrads

Venugopal Bandi,[a] Mohamed E. El-Khouly,[b, c] Kei Ohkubo,[b] Vladimir N. Nesterov,[a] Melvin E. Zandler,[d] Shunichi Fukuzumi,*[b, e] and Francis D'Souza*[a]

This paper is dedicated to Professor Maurizio Prato on the occasion of his 60th birthday

Abstract: Donor–acceptor distance, orientation, and photoexcitation wavelength are key factors in governing the efficiency and mechanism of electron-transfer reactions both in natural and synthetic systems. Although distance and orientation effects have been successfully demonstrated in simple donor–acceptor dyads, revealing excitation-wavelength-dependent photochemical properties demands multimodular, photosynthetic-reaction-center model compounds. Here, we successfully demonstrate donor–acceptor excitation-wavelength-dependent, ultrafast charge separation and charge recombination in newly synthesized, novel tetrads featuring bisferrocene, BF_2-chelated azadipyrromethene, and fullerene entities. The tetrads synthesized using multistep synthetic procedure revealed characteristic optical, redox, and photo reactivities of the individual components and featured "closely" and "distantly" positioned donor–acceptor systems. The near-IR-emitting BF_2-chelated azadipyrromethene acted as a photosensitizing electron acceptor along with fullerene, while the ferrocene entities acted as electron donors. Both tetrads revealed excitation-wavelength-dependent, photoinduced, electron-transfer events as probed by femtosecond transient absorption spectroscopy. That is, formation of the Fc^+–ADP–$C_{60}^{\bullet-}$ charge-separated state upon C_{60} excitation, and Fc^+–$ADP^{\bullet-}$–C_{60} formation upon ADP excitation is demonstrated.

Keywords: artificial photosynthesis · electron transfer · fullerenes · photochemistry · X-ray analysis

Introduction

An increase in global energy demand and fading natural resources has lead scientists to focus their attention on the development of environmentally clean alternative energy resources.[1,2] Specific emphasis has been placed on solar-energy harvesting, for which photocatalysis for the production of clean fuels by mimicking the natural photosynthesis[3] using electron donor–acceptor based molecular/supramolecular assemblies are often targeted.[4–9] In building such assemblies, exploration of new electron-donor and electron-acceptor molecules with absorption covering different parts of the electromagnetic spectrum (wide-band capture) and well-tuned redox states are realized to be key factors. Proper matching of spectral and redox states are expected to result in fast and efficient electron-transfer events. In addition, the presence of multiple photoactive entities covering absorption in different parts of the spectrum is expected to provide excitation-wavelength-dependent, photochemical events, useful for building wide-band light-energy-harvesting and optoelectronic devices.[10]

Among the newly established sensitizers, BF_2-chelated azadipyrromethene (abbreviated as ADP or aza-BODIPY),[11] a structural analogue of BF_2-chelated dipyrromethene (BODIPY),[12] has recently gained much attention for its photochemical properties. ADP absorbs in the 300–700 nm region with very high molar absorptivities, and desirable emission in the red region (660–700 nm) with quantum yields exceeding 40%.[13] Interestingly, the facile reduction of ADP makes it a rarely encountered electron-acceptor

[a] V. Bandi, Dr. V. N. Nesterov, Prof. F. D'Souza
Department of Chemistry, University of North Texas
1155 Union Circle, #305070, Denton
TX 76203-5017 (USA)
Fax: (+1) 940-565-4318
E-mail: Francis.DSouza@unt.edu

[b] Dr. M. E. El-Khouly, Dr. K. Ohkubo, Prof. S. Fukuzumi
Department of Material and Life Science
Graduate School of Engineering
Osaka University, Suita, Osaka 565-0871 (Japan)
Fax: (+81) 6-6879-7370
E-mail: fukuzumi@chem.eng.osaka-u.ac.jp

[c] Dr. M. E. El-Khouly
Department of Chemistry, Faculty of Science
Kafr ElSheikh University (Egypt)

[d] Prof. M. E. Zandler
Department of Chemistry, Wichita State University
Wichita, KS 67260-0051 (USA)

[e] Prof. S. Fukuzumi
Department of Bioinspired Science
Ewha Womans University, Seoul 120-750 (Korea)

Supporting information for this article is available on the WWW under http://dx.doi.org/10.1002/chem.201204317.

photosensitizer molecule.[14] Other electron-acceptor photosensitizers include fullerene and perylene diimide or naphthalene diimide derived compounds.[4–9] However, none of these emit in the near-IR region with high fluorescence quantum yields, thus making ADP a novel type of electron-deficient photosensitizer.

In an attempt to explore the novel features of ADP in photoinduced events related to light-energy conversion, recently, we reported the synthesis and characterization of a few donor–acceptor dyads and triads. Briefly, when ADP was connected to ferrocene, efficient photoinduced electron transfer from ferrocene to singlet-excited ADP was observed.[14] Alternatively, when C_{60} was covalently linked to ADP, the formation of $ADP^{\bullet+}$-$C_{60}^{\bullet-}$ was observed.[15] Excitation transfer was observed when either chlorophyll derivatives or BODIPY was covalently linked to ADP.[16] Interestingly, when a bisporphyrin was covalently linked to ADP, the resulting "molecular clip" supramolecularly assembled C_{60} through metal–ligand coordination. In this supramolecular assembly, control over energy- and electron-transfer events was accomplished.[17a] Furthermore, by using a combination of zinc porphyrin, BODIPY, and azaBODIPY, a novel broad-band, capturing and emitting, supramolecular triad useful for energy harvesting and building optoelectronic devices, was recently reported.[17b] Supramolecular donor–acceptor hybrids of zinc–phthalocyanine–ADP and zinc–naphthalocyanine–ADP, that is, near-IR-absorbing entities, were recently constructed to observe photoinduced electron transfer in the near-IR region.[17c]

In our continued effort to unravel the electron and energy donor and acceptor behavior of ADP-derived higher analogue supramolecular systems, we have designed novel tetrads featuring bisferrocene, ADP, and fullerene entities, positioned at different distances, as shown in Figure 1. Here, the near-IR emitting BF_2-chelated azadipyrromethane acts as a photosensitizing electron acceptor along with fullerene, while the ferrocene entities act as electron donors. Compounds **1** and **2** in Figure 1 represent the first set of tetrads derived from the near-IR-emitting ADP sensitizer to-date. This sensitizer could take important role in harvesting light energy of the red-region of the spectrum. Femtosecond transient absorption spectroscopy among other methods has been employed to unravel excitation-wavelength-dependent, ultrafast, electron-transfer events in these tetrads.

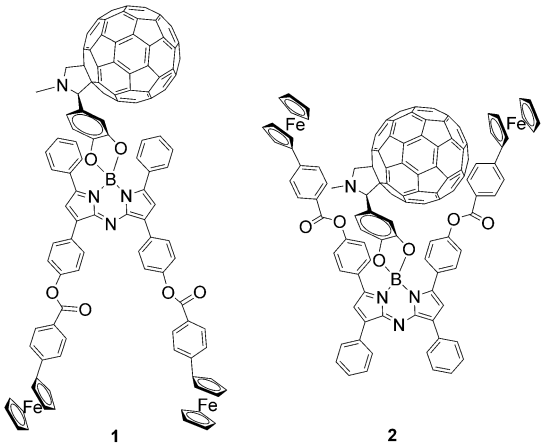

Figure 1. Structure of the newly synthesized distantly and closely spaced bisferrocene–ADP–fullerene molecular tetrads.

Results and Discussion

Synthesis of the tetrads: Scheme 1 summarizes the syntheses of tetrad, **1**, details of the syntheses are given in the experimental section. The multistep synthesis of **1** involved first,

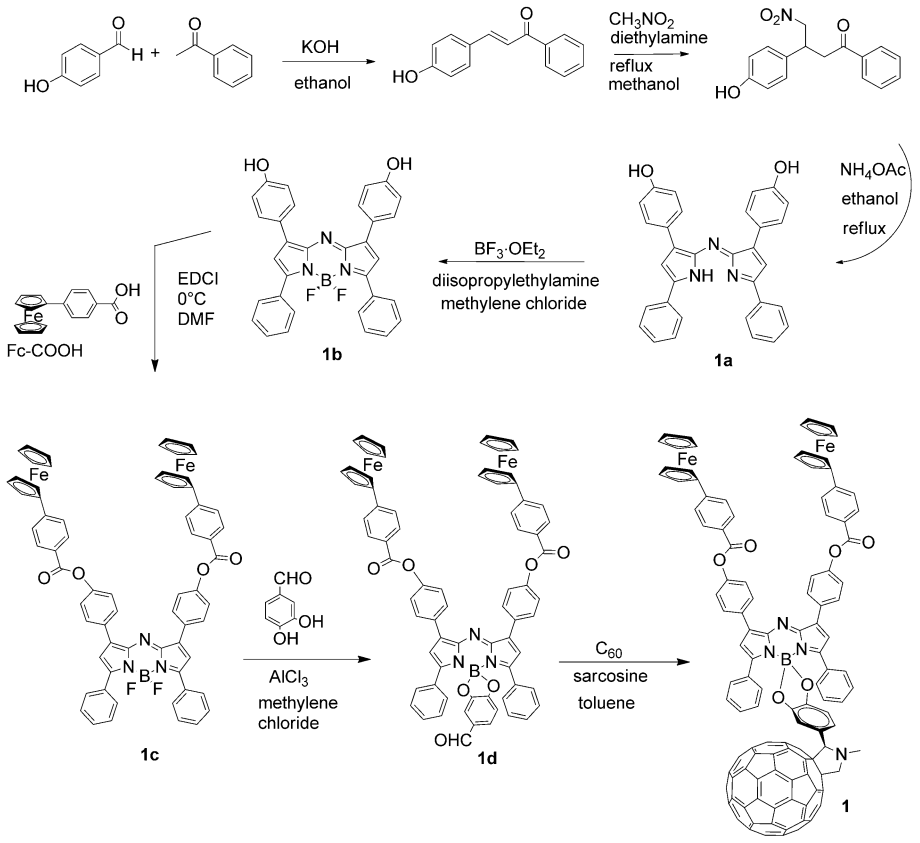

Scheme 1. Synthetic methodology developed for tetrad, 1.

synthesis of 3-(4-hydroxyphenyl)-1-phenylprop-2-en-1-one from a reaction of the corresponding 4-hydroxybenzaldehyde, acetophenone, and potassium hydroxide. This was subsequently reacted with nitromethane and diethylamine in dry ethanol to obtain 3-(4-hydroxyphenyl)-4-nitro-1-phenylbutan-1-one. The 4-{2-[3-(4-hydroxyphenyl)-5-phenyl-1*H*-pyrrolylimino]-5-phenyl-2*H*-pyrrol-3-yl}phenol (**1a**) was synthesized by reacting it with ammonium acetate in ethanol. Next, BF_2-chelated 4-{2-[3-(4-hydroxyphenyl)-5-phenyl-1*H*-pyrrol-2ylimino]-5-phenyl-2*H*-pyrrol-3-yl}phenol (**1b**), was formed from **1a**, by treating it with diisopropylethylamine and boron trifluoride diethyl etherate in dry CH_2Cl_2. The bisferrocene–ADP triad, **1c** was obtained by reactions of **1b** with appropriate amounts of 4-ferrocenyl benzoic acid in the presence of 1-ethyl-3-(3-dimethylaminopropyl)carbodiimide (EDCI) followed by chromatographic purification. This compound was further reacted with 3,4-dihydroxybenzaldehyde in the presence of $AlCl_3$ to obtain the formyl phenyl dioxyboron derivative, **1d**. Finally, fullerene was appended by reacting **1d** with fullerene and *N*-methylglycine in toluene to obtain tetrad, **1**.

The synthesis of tetrad **2** is shown in Scheme 2, while details are given in the Experimental Section. The structural integrity of the newly synthesized compounds was established from ^{1}H NMR spectroscopy, MALDI-TOF MS, and optical techniques.

X-ray structural studies: In the present study, we have also been able to solve the structures of two of the precursor compounds involved in the complex syntheses of the tetrads, namely, the free-base versions of (3,5-diphenyl-1*H*-pyrrol-2-yl)(3,5-diphenylpyrrol-2-ylidene)amine (**1a** and **2a** without hydroxyl groups) and BF_2-chelated [5-(4-hydroxyphenyl)-3-phenyl-1*H*-pyrrol-2-yl]-[5-(4-hydroxyphenyl)-3-phenylpyrrol-2-ylidene] amine (**2b**).

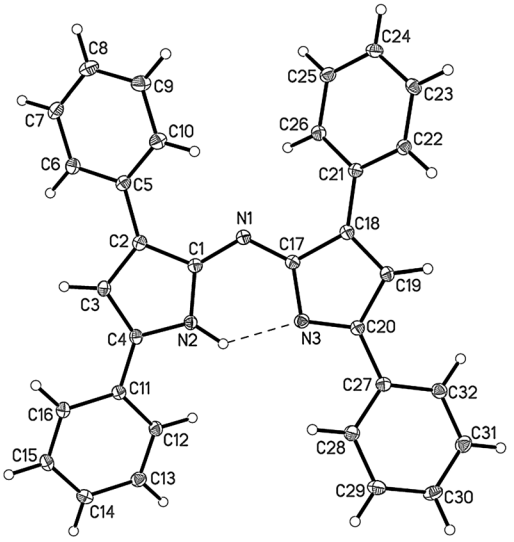

Figure 2. Projection diagram of (3,5-diphenyl-1*H*-pyrrol-2-yl)(3,5-diphenylpyrrol-2-ylidene)amine with 50% thermal ellipsoids. Dashed line shows intramolecular N–H···N hydrogen bond.

The X-ray structure of the former compound is shown in Figure 2. The molecule crystallized in the triclinic crystal system.[18] The macrocycle assumed the position suitable for subsequent boron chelation, perhaps facilitated by the N–H···N intramolecular hydrogen bond. No notable intermolecular interactions between the molecules in the crystal packing were observed. The crystal packing diagram (Figure S1), atomic coordinates and anisotropic displacement parameters (Tables S1, S3 and S4), bond lengths, angles, and hydrogen bonds (Tables S2 and S5) are given in the Supporting Information.

The X-ray structure of **2b** is shown in Figure 3. The molecule crystallized in the orthorhombic crystal system.[19] The boron assumes a tetrahedral geometry with the two ring nitrogen atoms and two fluorine atoms. Some intermolecular interactions were also observed in the crystal packing. The crystal packing diagram (Figure S2), atomic coordinates and anisotropic displacement parameters (Tables S6, S8 and S9), bond lengths, angles, and hydrogen bonds (Tables S7 and S10) are given in the Supporting Information.

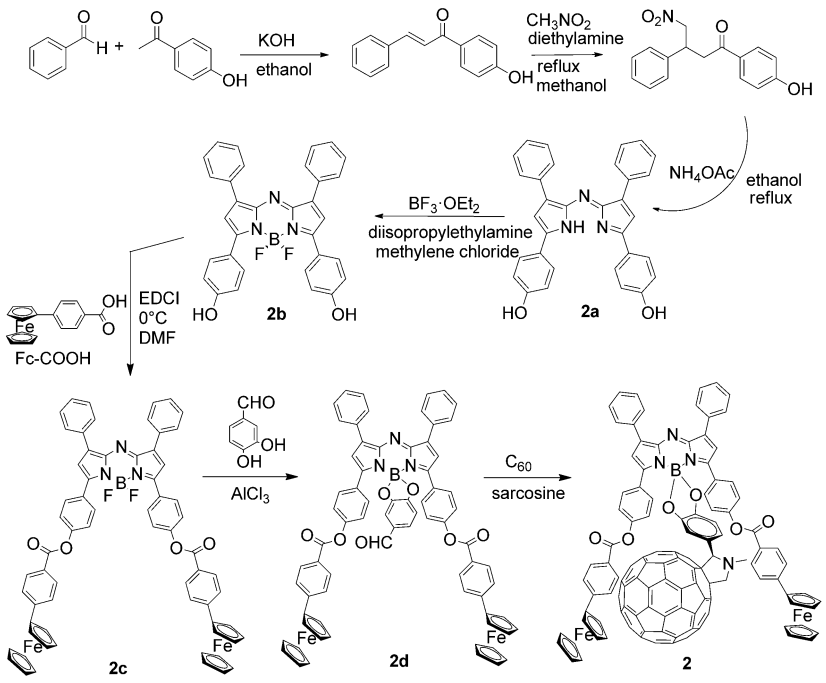

Scheme 2. Synthetic methodology developed for tetrad, **2**.

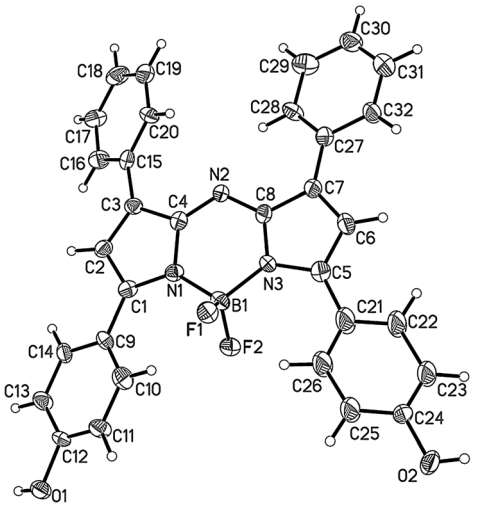

Figure 3. Projection diagram of **2b** with 50% thermal ellipsoids. Disordered part of the molecule (C22B···C26B) is omitted for clarity.

Absorption and emission studies: Absorption spectra of the tetrads **1** (Figure 4a) and **2** (Figure 4c) revealed optical features involving all of the three entities. Bands corresponding to ADP were recorded at 300, 475, and 635 nm. The ferrocene peak was overlapped with the 300 nm band of ADP, while the fullerene peak also overlapped with this band, along with a sharp peak at 432 nm characteristic of fulleropyrrolidine. Importantly, the ADP peaks were found to be blue-shifted by 15–20 nm corresponding to their controls (**1b**, **1c**, **2b**, and **2c**) as a result introducing ferrocene and fullerene entities. Additionally, conversion of the BF_2 functionality of **1c** and **2c** into BO_2 in **1** and **2** contributed to this cause. The ADP emission of **1b** and **2b** was observed at 720 and 735 nm, respectively (see Figure 4b and d). The two hydroxyl groups of **1b** and **2b** redshifted the emission maxima from the original emission peak of ADP (without −OH groups) at 682 nm in benzonitrile.[14] Presence of either ferrocene or fullerene or both of these entities in **1** and **2** quantitatively quenched the ADP emission indicating occurrence of photochemical events.[20]

Electrochemistry and energy levels: To establish the energy levels, electrochemical studies using cyclic voltammetry (CV) were performed on both the tetrads (Figure 5). The site of electron transfer was arrived using control compounds of monomeric species, namely, phenyl ferrocene, ADP, and fulleropyrrolidine. The cyclic voltammogram of **1** revealed reduction peaks at $E_{1/2} = -0.37$, -0.63, and -1.02 V vs. Ag/AgCl (Figure 5a). By comparison, the first reversible reduction has been attributed to the reduction of ADP macrocycle, while the second reduction to the reduction of fullerene spheroid. The third reduction wave was an overlap of

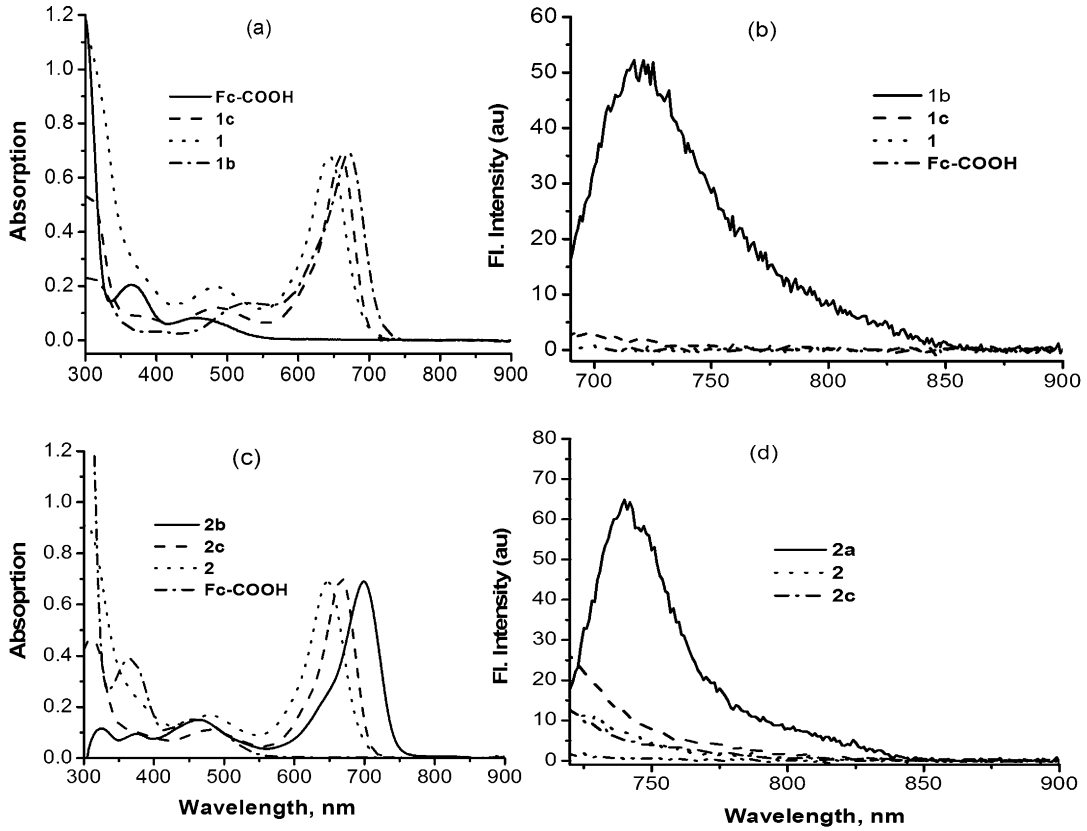

Figure 4. Optical absorption (a and c) and fluorescence emission (b and d) spectra of the indicated compounds in benzonitrile (see Scheme 1 for structures). $\lambda_{ex} = 671$ nm for **1** and 699 nm for **2**.

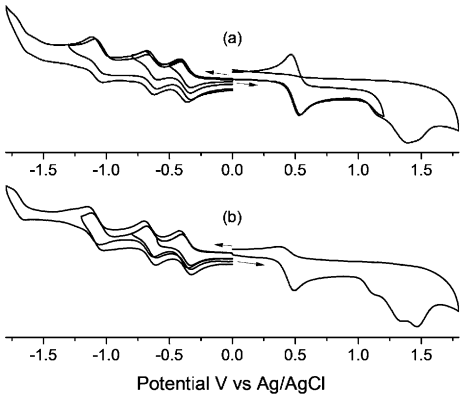

Figure 5. Cyclic voltammograms of tetrads a) **1** and b) **2** in benzonitrile containing 0.1 M $(TBA)ClO_4$. The potentials are referenced to Ag/AgCl. Scan rate = 100 mV s^{-1}.

the second reduction of ADP and fullerene entities. In agreement with our previous report,[15] the easy reduction of ADP compared to fullerene was evident from these studies. During oxidation, reversible processes at $E_{1/2} = 0.49$ V vs. Ag/AgCl corresponding to ferrocene oxidation and one or more irreversible oxidations beyond 1.14 V corresponding to ADP oxidation were observed. The current for ferrocene oxidation was twice as that of C_{60} reduction. Similar observations were also made for tetrad **2** (Figure 5b). The data of redox potentials are summarized in Table 1.

Table 1. Redox potentials (V vs. Ag/AgCl) of **1** and **2** in deaerated PhCN containing $(TBA)ClO_4$ (0.1 M).

	$C_{60}^{2-}/C_{60}^{\bullet-}$ $ADP^{2-}/ADP^{\bullet-}$	$C_{60}^{\bullet-}/C_{60}$	$ADP^{\bullet-}/ADP$	Fc^{+}/Fc	$ADP^{\bullet+}/ADP$
1	−1.02	−0.63	−0.37	0.49	1.14[a]
2	−1.04	−0.64	−0.36	0.44	1.12[a]

[a] Peak potential with the scan rate of 100 mV s^{-1}.

The structure of the tetrads was visualized by performing computational calculations at the B3LYP/3-21G(*) level.[21,22] Figure 6 shows optimized structures on the Born–Oppenheimer potential-energy surface for both tetrads. For

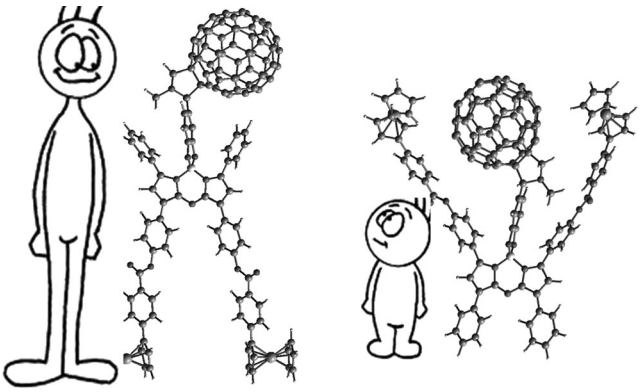

Figure 6. B3LYP/3-21G(*) optimized structures and cartoons showing tall (distant) and short (close) versions of tetrads **1** and **2**.

tetrad **1** with distinctly positioned entities, the length of the molecule measured as the carbon–carbon distance of furthest ferrocene and fullerene entities was about 32.2 Å, while this distance for tetrad **2** with closely positioned entities was about 21.7 Å, that is, over 10 Å increase in length for the former tetrad. The center-to-center distances between B–Fe, B–C_{60}, and Fe–C_{60} were 16.7, 11.1, and 27.9 Å for **1** and 13.9, 11.5, and 8.2 Å for **2**. In case of **2**, the ferrocene carbon atom was as close as 3.9 Å from the nearby located fullerene carbon atom, suggesting some intramolecular interactions. However, no such intramolecular interactions were apparent in **1**.

The energies of the charge-separated states were calculated by using the redox, geometric, and optical data, according to the Weller approach.[23,24] By comparing the energy levels of the charge-separated states with the energy levels of the excited states, the driving forces of charge separation ($-\Delta G_{CS}$) were also evaluated. The generation of Fc^{+}–$ADP^{\bullet-}$–C_{60} ($-\Delta G_{CS} = 0.92$ eV for **1** and 0.94 eV for **2**) and Fc^{+}–ADP–$C_{60}^{\bullet-}$ ($-\Delta G_{CS} = 0.63$ eV for **1** and 0.67 eV for **2**) was found to be exergonic via the singlet excited state of ADP in benzonitrile. Based on the redox potential measurements, the formation of $ADP^{\bullet-}$-$C_{60}^{\bullet+}$ (ca. 1.8 eV) is excluded, because of its higher energy compared with the ^{1}ADP* (1.78 eV for **1** and 1.73 eV for **2**) and $^1C_{60}$* (1.75 eV) excited states.[14,15]

Photodynamics probed by femtosecond transient spectroscopy: The photodynamics of the tetrads and the control compounds via the singlet ADP was examined by femtosecond transient measurements by using the excitation at 400 nm for the fullerene moiety, as shown in Figure 7. The transient spectra of both **1** and **2** exhibited bands at 1000 nm corresponding to $C_{60}^{\bullet-}$, suggesting formation of Fc^{+}–ADP–$C_{60}^{\bullet-}$ radical–ion pair as charge-separated states. These spectral features were different from the control compounds, **1c** and **2c**, given in Figure S3 and S4 in the Supporting Information. The rate constants of charge separation (k_{CS}) measured from the decay of the ^{1}ADP* were determined to be 3.2×10^{11} and 3.8×10^{11} s^{-1} for **1** and **2**, respectively, indicating occurrence of efficient electron transfer from Fc to $^1C_{60}$* and yielding the charge-separated states Fc^{+}–ADP–$C_{60}^{\bullet-}$ (see Figures S5 and S6 in the Supporting Information for decay profiles); however, it should be kept in mind that the CS from ADP to $^1C_{60}$* is energetically unfavorable [ΔG ca. +0.05 eV obtained from the one-electron reduction and oxidation potentials of C_{60} and ADP (vide supra)]. It should also be noted that the absorption bands of Fc^{+} were not detected in Figure 5 due to its low extinction coefficient. The rate constants of charge recombination (k_{CR}) were determined to be 1.1×10^{10} and 8.4×10^{10} s^{-1} (lifetime: 88 and 12 ps) for **1** and **2**, respectively. The charge recombination in the charge-separated state of **1** and **2** may proceed by means of electron transfer from $C_{60}^{\bullet-}$ to ADP, followed by rapid electron transfer from $ADP^{\bullet-}$ to Fc^{+} (vide infra). However, the much shorter lifetime of the charge-separated state of **2** suggests the occurrence of direct back-electron transfer

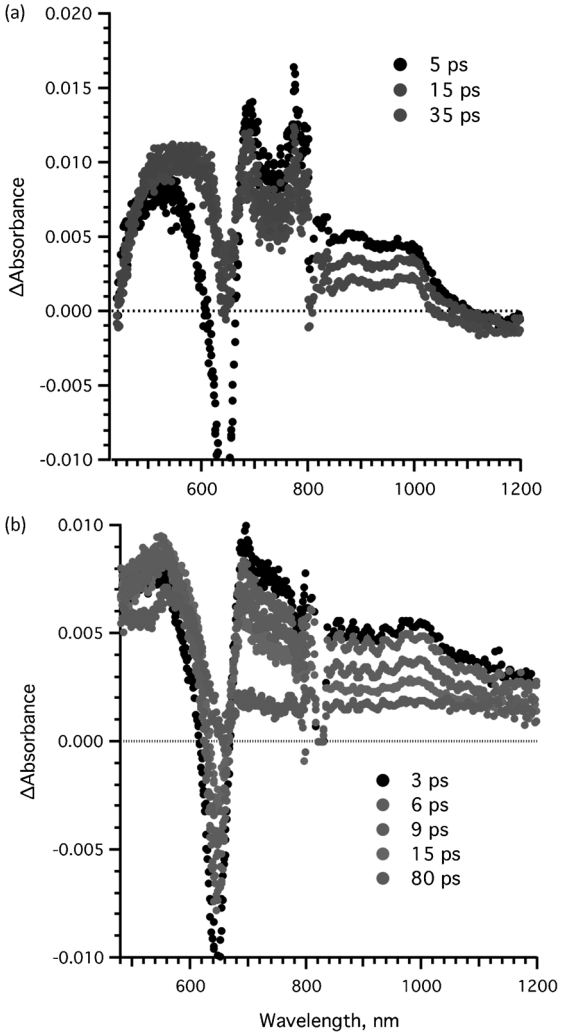

Figure 7. Femtosecond transient absorption spectra of a) **1** and b) **2** in deaerated benzonitrile. $\lambda_{ex} = 400$ nm.

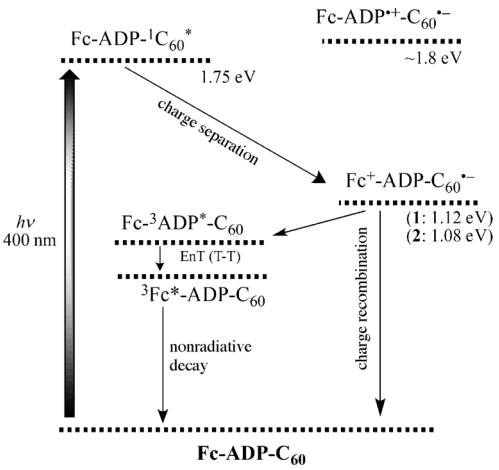

Scheme 3. Energy diagram of Fc–ADP–C_{60} for the excitation of the C_{60} moiety.

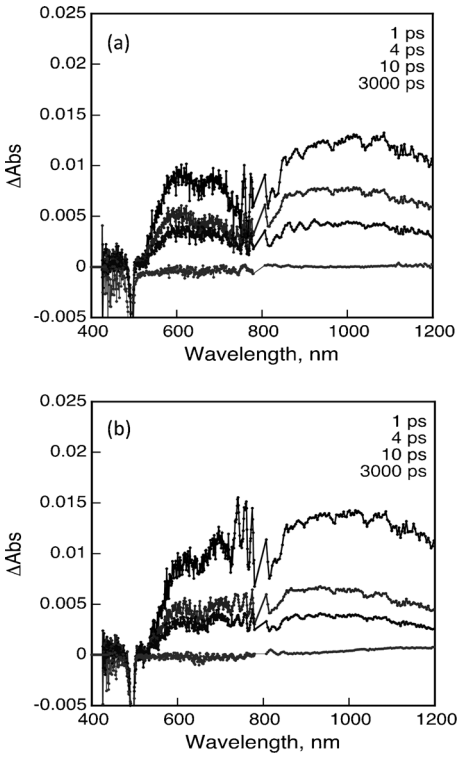

Figure 8. Femtosecond transient absorption spectra of **1** (top panel) and **2** (bottom panel) in deaerated benzonitrile. $\lambda_{ex} = 480$ nm.

from $C_{60}^{\bullet-}$ to Fc^+ owing to the shorter distance between Fc and C_{60} in **2** as compared with **1** (Figure 5).[25] The complementary nanosecond transient spectra (see Figure S7 in the Supporting Information) showed extremely weak absorption of the triplet ADP in the 500–600 nm region. This observation suggests that 1) the charge recombination takes place to populate the ground state and/or 2) the charge recombination takes place to populate the triplet ADP (ca. 1 eV), which is rapidly quenched by the low-lying triplet Fc.[26] The proposed energy diagram for photochemical events occurring upon excitation of the C_{60} moiety is summarized in Scheme 3.

In contrast, when the ADP entity was excited at 480 nm by femtosecond laser flash photolysis, no absorption band due to $C_{60}^{\bullet-}$ was observed at 1000 nm as shown in Figure 8. The transient absorption bands at 620 and 800–1200 nm observed at 1 ps are assigned to the singlet excited state of ADP. The decay rate constants were determined to be 5.5×10^{10} and 9.0×10^{10} s^{-1} for **1** and **2**, respectively (see Figure S8 in the Supporting Information). ^{1}ADP* is efficiently quenched by the Fc moiety by electron transfer from Fc to ^{1}ADP*. However, no charge-separated state was observed because the rate of charge recombination bound for the ground state seems to be faster than that of photoinduced electron transfer. In addition, no clear evidence of energy transfer from the singlet excited ADP to fullerene was observed. The proposed energy diagram for photochemical events occurring upon excitation of the ADP moiety is summarized in Scheme 4.

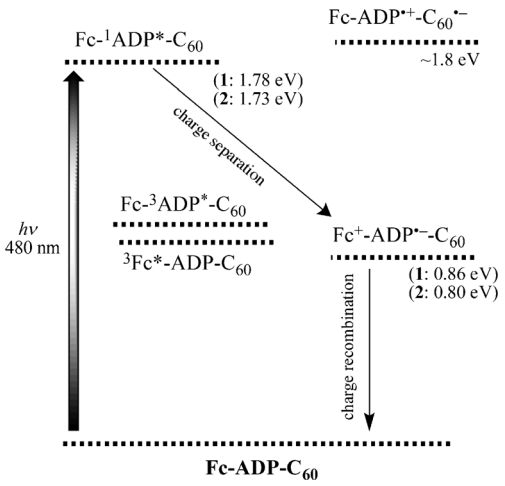

Scheme 4. Energy diagram of Fc–ADP–C_{60} for the excitation of the ADP moiety.

Conclusion

Tetrads featuring near-IR-emitting ADP as an electron-acceptor sensitizer, ferrocene as the primary electron donor, and fullerene as a second electron acceptor have been designed and synthesized. The positions of different entities are controlled such a way that two tetrads are obtained, one in which the ferrocene and fullerene entites are in close proximity and the other in which they are far apart. As expected from the free-energy calculations involving redox potentials and geometry parameters, excitation-wavelength-dependent, ultrafast, photoinduced electron transfer events have been witnessed. That is, when C_{60} was excited, formation of an Fc^+–ADP–$C_{60}^{\bullet-}$ radical–ion pair was evidenced, for which the spatial separation of the entities played a significant role in governing the kinetics of electron transfer. Interestingly, excitation of the near-IR probe, ADP, in the tetrads resulted in ultrafast charge separation and recombination involving ferrocene but not C_{60}. Further studies, replacing the electron-donor ferrocene with other well-known electron donors, to visualize the novel wavelength-dependent photochemical events of tetrads featuring near-IR-emitting ADP electron-acceptor sensitizer and the associated mechanistic details are in progress.

Experimental Section

Chemicals: Buckminsterfullerene, C_{60} (+99.95%) was from SES Research, (Houston, TX). All the reagents were from Aldrich Chemicals (Milwaukee, WI) while the bulk solvents utilized in the syntheses were from Fischer Chemicals. The tetra-*n*-butylammonium perchlorate [(TBA)ClO_4] used in electrochemical studies was from Fluka Chemicals.

Procedure for synthesis of Fc_2–azaBODIPY–C_{60} (1)

3-(4-Hydroxyphenyl)-1-phenylprop-2-en-1-one: 4-Hydroxybenzaldehyde (5 g, 4×10^{-2} mol), acetophenone (4.91 g, 4×10^{-2} mol) and potassium hydroxide (0.07 g, 1.2×10^{-3} mol) were dissolved in ethanol/water (85:15 v/v, 100 cm^3) and stirred at room temperature for a period of 24 h. The reaction mixture was allowed to cool in ice–water bath, during which the product precipitated. Filtration of the reaction mixture gave a pale white solid product. Yield: 3.60 g (40%).

3-(4-Hydroxyphenyl)-4-nitro-1-phenylbutan-1-one: 3-(4-Hydroxyphenyl)-1-phenylprop-2-en-1-one (3.6 g, 1.6×10^{-2} mol), nitromethane (9.79 g, 0.160 mol), and diethylamine (5.87 g, 0.08 mol) were dissolved in dry ethanol (54 cm^3) and heated under reflux for 24 h. The solution was cooled, acidified with 1.0 M HCl to precipitate the compound. Yield: 2 g (44%).

4-{2-[3-(4-hydroxyphenyl)-5-phenyl-1*H*-pyrrol-2-ylimino]-5-phenyl-2*H*-pyrrol-3-yl}phenol (1a): A solution of 3-(4-hydroxyphenyl)-4-nitro-1-phenylbutan-1-one (2 g, 7.01×10^{-3} mol) and ammonium acetate (18.92 g, 0.25 mol) in ethanol (80 cm^3) was heated under reflux for 24 h. During the course of the reaction, the product precipitated as blue-black solid. The reaction was allowed to cool to room temperature and solid was filtered and washed with ethanol to give the product: Yield: 0.5 g (15%); ^{1}H NMR (400 MHz, $CDCl_3$): $\delta=8.00$–7.78 (m, 6H), 7.36–7.50 (m, 8H), 7.02–7.06 (s, 2H), 6.74–6.84 ppm (d, $J=16$ Hz, 4H).

BF_2 chelate of 4-{2-[3-(4-hydroxyphenyl)-5-phenyl-1*H*-pyrrol-2-ylimino]-5-phenyl-2*H*-pyrrol-3-yl}phenol (1b): Compound **1a** (0.5 g, 1.03×10^{-3} mol) was dissolved in dry CH_2Cl_2 (200 cm^3). Diisopropylethylamine (1.36 g, 0.01 mol) and boron trifluoride diethyl etherate (2.66 g, 0.0187 mol) were added and the mixture was stirred at room temperature under N_2 for 24 h. The mixture was washed with water and the organic layer was separated, dried over Na_2SO_4, and evaporated to dryness. The residue was purified by column chromatography on silica gel with CH_2Cl_2/ethyl acetate 4:1 to give metallic red solid: Yield: 0.3 g (54%); ^{1}H NMR (400 MHz, $CDCl_3$): $\delta=8.04$–8.00 (m, 8H), 7.46–7.50 (m, 6H), 6.94–6.96 (s, 2H), 6.90–6.93 ppm (t, $J=8$ Hz, 4H); MS(MALDI-TOF); *m*/*z* calcd for $C_{32}H_{22}BF_2N_3O_2$: 529.18; found: 528.12; UV/Vis: $\lambda_{max}=671$ nm.

Fc_2–azaBODIPY (1c): 4-Ferrocenylbenzoic acid (333.6 mg, 1.08 mmol) was dissolved in DMF (20 cm^3), to which EDCI (250.70 mg, 1.3 mmol) was added at 0 °C under N_2, followed by the addition of compound **1b** (115.38 mg, 0.2 mmol), after which the mixture was stirred for 24 h. Then the solvent was removed under reduced pressure. The residue was dissolved in CH_2Cl_2 and the mixture was washed with water. The organic layer was separated, dried over Na_2SO_4 and solvent was evaporated. The residue was purified by column chromatography on silica gel with CH_2Cl_2/hexanes (1:1) to give compound **1c**. Yield: 15 mg (6%); ^{1}H NMR (400 MHz, $CDCl_3$): $\delta=8.20$–8.10 (m, 8H), 8.12–7.90 (d, $J=8$ Hz, 4H), 7.60–7.46 (d, $J=8$ Hz, 8H), 7.40–7.30 (m, 6H), 7.10–7.00 (s, 2H), 4.88–4.70 (t, $J=4$ Hz, 4H), 4.50–4.60 (t, $J=4$ Hz, 4H), 4.20–4.00 ppm (m, 10H); UV/Vis: $\lambda_{max}=655$ nm.

Fc_2–azaBODIPY–aldehyde (1d): Compound **1c** (0.1 g, 0.10 mmol) was dissolved in dry CH_2Cl_2 (20 cm^3) and stirred under argon for 10 min. Then $AlCl_3$ (18 mg, 0.135 mmol) was added and the solution was further stirred for 15 min before addition of 3,4-dihydroxybenzaldehyde (18.7 mg, 0.135 mmol). The mixture was stirred for 20 min and the solvent was evaporated under reduced pressure. The crude product was purified by column chromatography (deactivated basic alumina) with CH_2Cl_2/hexanes 3:1 to give the product. Yield: 0.050 g (41%); ^{1}H NMR (400 MHz, $CDCl_3$): $\delta=9.60$–9.54 (s, 1H), $\delta=8.20$–8.10 (m, 8H), $\delta=8.12$–7.90 (d, $J=8$ Hz, 4H), 7.60–7.48 (d, $J=16$ Hz, 6H), 7.46–7.30 (m, 8H), 7.00–6.84 (m, 3H), 6.90–6.80 (s, 2H), 4.88–4.70 (t, $J=4$ Hz, 4H), 4.50–4.60 (t, $J=4$ Hz, 4H), 4.20–4.00 ppm (m, 10H).

Fc_2–azaBODIPY–C_{60}, (1): Sarcosine (0.018 g, 2.07×10^{-4} mmol) and compound **1d** (0.050 g, 4.15×10^{-5} mmol) were added to a solution of C_{60} (0.89 g, 1.24×10^{-4} mmol), in dry toluene (100 cm^3). The solution mixture was refluxed for 24 h and the solvent was removed under vacuum. The residue was purified by column chromatography (silica) with 1:4 ethyl acetate/CH_2Cl_2 as eluent to give the product. Yield: 0.030 g (42%); ^{1}H NMR (400 MHz, $CDCl_3$): $\delta=8.20$–8.04 (m, 12H), 7.60–7.50 (m, 4H), 7.40–7.30 (m, 9H), 6.94–6.99 (s, 2H), 6.86–6.76 (m, 4H), 4.90–4.82 (d, $J=7$ Hz, 1H), 4.80–4.70 (t, $J=8$ Hz, 4H), 4.50–4.60 (s, 1H), 4.50–4.40 (t, $J=8$ Hz, 4H), 4.30–4.20 (s, 1H), 4.18–4.10 (m, 10H), 2.60–2.48 ppm (s, 3H); UV/Vis $\lambda_{max}=640$ nm; MALDI-TOF-MS (dithranol): *m*/*z* calcd for $C_{135}H_{55}BFe_2N_4O_6$: 1951.29; found: 1951.30 (see Figure S6 in the Supporting Information).

Procedure for synthesis of Fc_2–azaBODIPY–C_{60} tetrad (2)

1-(4-Hydroxyphenyl)-3-phenylpropenone: Benzaldehyde (2.1 g, 2×10^{-2} mol) 4-hydroxy acetophenone (2.69 g, 2×10^{-2} mol) and potassium hydroxide (0.03 g, 6×10^{-4} mol) were dissolved in ethanol/water (85:15 v/v, 100 cm^3) and stirred at room temperature for a period of 24 h. The reaction mixture was allowed to cool in ice–water bath during which the product precipitated. Filtration of the reaction mixture gave a pale white solid product. Yield: 3.81 g (85%); ^{1}H NMR (400 MHz, $CDCl_3$): $\delta=7.99$ (m, 2H), 7.77 (m, 1H), 7.60, (m, 2H), 7.5 (m, 1H), 7.39 (m, 3H), 6.9 ppm (m, 2H).

1-(4-Hydroxyphenyl)-4-nitro-3-phenylbutan-1-one: 1-(4-Hydroxyphenyl)-3-phenyl propenone (5.0 g, 2.2×10^{-2} mol), nitromethane (13.61 g, 0.223 mol), and diethylamine (8.12 g, 0.111 mol) were dissolved in dry ethanol (35 cm^3) and heated under reflux for 24 h. The solution was cooled, acidified with 1 M HCl to precipitate the compound. Yield: 4.58 g (72%); ^{1}H NMR (400 MHz, $CDCl_3$): $\delta=7.82$ (d, $J=8$ Hz, 2H), 7.2 (m, 5H), 6.8 (d, $J=7$ Hz, 2H), 4.8 (m, 1H), 4.62 (m, 1H), 4.15 (m, 1H), 3.35 ppm (m, 2H).

[5-(4-Hydroxyphenyl)-3-phenyl-1*H*-pyrrol-2-yl]-[5-(4-hydroxyphenyl)-3-phenylpyrrol-2-ylidene]amine (2a): A solution of 1-(4-hydroxyphenyl)-4-nitro-3-phenylbutan-1-one (5 g, 1.8×10^{-2} mol) and ammonium acetate (47.31 g, 0.61 mol) in ethanol (125 cm^3) was heated under reflux for 24 h. During the course of the reaction, the product precipitated as blue-black solid. The reaction was allowed to cool to room temperature and solid was filtered and washed with ethanol to give the product. Yield: 2.16 g (51%); ^{1}H NMR (400 MHz, $CDCl_3$): $\delta=8.04$ (d, $J=8$ Hz, 4H), 7.84 (d, $J=7$ Hz, 4H), 7.32 (m, 6H), 7.12 (s, 2H), 6.98 ppm (d, $J=8$ Hz, 4H).

BF_2 chelate of [5-(4-hydroxyphenyl)-3-phenyl-1*H*-pyrrol-2-yl]-[5-(4-hydroxyphenyl)-3-phenylpyrrol-2-ylidene]amine (2b): Compound **2a** (1 g, 2.07 mmol) was dissolved in dry CH_2Cl_2 (100 cm^3). Diisopropylethylamine (2.71 g, 2.1×10^{-2} mol) and boron trifluoride diethyl etherate (5.32 g, 0.037 mol) were added and the mixture was stirred at room temperature under N_2 for 24 h. The mixture was washed with water and the organic layer was separated, dried over Na_2SO_4 and evaporated to dryness. The residue was purified by column chromatography on silica gel with CH_2Cl_2/ethyl acetate 4:1 to give metallic red solid. Yield: 0.76 g (69%); ^{1}H NMR (400 MHz, $CDCl_3$): $\delta=8.1$ (m, 8H), 7.35 (m, 6H), 7.18 (s, 2H), 6.9 ppm (m, 4H) ppm; MS(MALDI-TOF): *m/z* calcd for $C_{32}H_{22}BF_2N_3O_2$: 529.18; found: 529.39; UV/Vis: $\lambda_{max}=699$ nm.

Fc_2–azaBODIPY (2c): 4-Ferrocenylbenzoic acid (289.17 mg, 0.94 mmol) was dissolved in DMF (20 cm^3), to which EDCI (217.28 mg, 1.13 mmol) was added at 0 °C under N_2, followed by the addition of compound **2b** (100 mg, 0.2 mmol), after which the mixture was stirred for 24 h. Then the solvent was removed under reduced pressure. The residue was dissolved in CH_2Cl_2 and the mixture was washed with water. The organic layer was separated and dried over Na_2SO_4 and the solvent was evaporated. The residue was purified by column chromatography on silica gel with CH_2Cl_2/hexanes (1:1) to give compound **2c**. Yield: 50 mg (50%); ^{1}H NMR (400 MHz, $CDCl_3$): $\delta=8.20$–8.04 (m, 12H), 7.60–7.50 (m, 4H), 7.50–7.40 (m, 6H), 7.42–7.30 (d, $J=6$ Hz, 4H) 7.10–7.00 (s, 2H), 4.80–4.70 (t, $J=1.6$ Hz, 4H), 4.50–4.40 (t, $J=3.2$ Hz, 4H), 4.18–4.10 (m, 10H); UV/Vis: $\lambda_{max}=670$ nm.

Fc_2–azaBODIPY–aldehyde (2d): Compound **2c** (0.1 g, 0.10 mmol) was dissolved in dry CH_2Cl_2 (20 cm^3) and stirred under argon for 10 min. Then $AlCl_3$ (0.018 g, 0.135 mmol) was added and the solution was further stirred for 15 min before addition of 3,4-dihydroxybenzaldehyde (0.018 g, 0.135 mmol). The mixture was stirred for 20 min and the solvent was evaporated under reduced pressure. The crude product was purified by column chromatography (deactivated basic alumina) with CH_2Cl_2/hexanes 3:1 to give the product. Yield: 0.077 g (64%); ^{1}H NMR (400 MHz, $CDCl_3$): $\delta=9.65$–9.70 (s, 1H), 8.15–8.06 (m, 8H), 8.02–7.98 (d, $J=8$ Hz, 4H), 7.58–7.52 (m, $J=8$ Hz, 4H), 7.50–7.43 (m, 6H), 7.38–7.32 (d, $J=8$ Hz, 4H), 6.86–6.78 (m, 3H), 6.68–6.62 (d, $J=4$ Hz, 1H), 6.32–6.28 (d, $J=8$ Hz, 1H), 4.78–4.70 (m, $J=7$ Hz, 4H), 4.44–4.38 (t, $J=4$ Hz, 4H), 4.00–4.06 (s, 10H).

Fc_2–azaBODIPY–C_{60} (2): Sarcosine (0.005 g, 6.2×10^{-5} mmol) and compound **2d** (0.015 g, 1.2×10^{-5} mmol) were added to a solution of C_{60} (0.026 g, 3.7×10^{-5} mmol), in dry toluene (100 cm^3). The solution mixture was refluxed for 24 h and the solvent was removed under vacuum. The residue was purified by column chromatography (silica) with 1:4 ethyl acetate/CH_2Cl_2 as eluent to give the product. Yield: 0.014 g (70%); ^{1}H NMR (400 MHz, $CDCl_3$) $\delta=8.02$–8.12 (m, 8H), 8.00–7.86 (d, $J=12$ Hz, 4H), 7.56–7.52 (d, $J=8$ Hz, 4H), 7.50–7.48 (m, 6H), 7.38–7.32 (d, $J=7$ Hz, 4H), 6.85–6.71 (m, 3H), 6.68–6.64 (d, $J=8$ Hz, 1H), 6.34–6.28 (d, $J=9$ Hz, 1H), 4.90–4.86 (d, $J=8$ Hz, 1H), 4.80–4.70 (m, $J=4$ Hz, 4H), 4.72–4.64 (s, 1H), 4.48–4.38 (m, $J=8$ Hz, 4H), 4.14–4.10 (d, $J=8$ Hz, 1H), 4.10–4.00 (m, 10H), 2.70–2.60 (s, 3H); UV/Vis: $\lambda_{max}=650$ nm; MALDI-TOF-MS (dithranol): *m/z* calcd for $C_{135}H_{55}BFe_2N_4O_6$: 1951.29; found: 1951.30 (see Figure S6 in the Supporting Information).

Instruments: The UV/Vis spectral measurements were carried out with a Shimadzu Model 2550 double monochromator UV/Vis spectrophotometer. The fluorescence emission was monitored by using a Varian Eclipse spectrometer. A right-angle detection method was used. The ^{1}H NMR studies were carried out on a Varian 400 MHz spectrometer. Tetramethylsilane (TMS) was used as an internal standard.

Crystal structure determination for compounds like **1a/2a** and **2b** was carried out using a Bruker SMATR APEX2 CCD-based X-ray diffractometer equipped with a low temperature device and Mo-target X-ray tube (wavelength = 0.71073 Å). Measurements were taken at 100(2) and 200 K, respectively.

Cyclic voltammograms were recorded on an EG&G PARSTAT electrochemical analyzer using a three-electrode system. A platinum button electrode was used as the working electrode, a platinum wire served as the counter electrode, and an Ag/AgCl electrode was used as the reference electrode. Ferrocene/ferrocenium redox couple was used as an internal standard. All the solutions were purged prior to electrochemical and spectral measurements using argon gas. MALDI-TOF spectra of the tetrads were recorded in dichloromethane with an Applied Biosystems Voyager-DE-STR using dithranol as a matrix (Supporting Information, Figure S9). The computational calculations were performed by DFT B3LYP/3–21G* methods with GAUSSIAN 09 software package[21] on high speed PCs.

Laser flash photolysis: The studied compounds were excited by a Panther OPO pumped by Nd:YAG laser (Continuum, SLII-10, 4–6 ns fwhm) with the powers of 1.5 and 3.0 mJ per pulse. The transient absorption measurements were performed using a continuous xenon lamp (150 W) and an InGaAs-PIN photodiode (Hamamatsu 2949) as a probe light and a detector, respectively. The output from the photodiodes and a photomultiplier tube was recorded with a digitizing oscilloscope (Tektronix, TDS3032, 300 MHz).

Femtosecond transient absorption spectroscopy experiments were conducted using an ultrafast source: Integra-C (Quantronix Corp.), an optical parametric amplifier: TOPAS (Light Conversion Ltd.) and a commercially available optical detection system: Helios provided by Ultrafast Systems LLC. The source for the pump and probe pulses were derived from the fundamental output of Integra-C (780 nm, 2 μJ per pulse and fwhm = 130 fs) at a repetition rate of 1 kHz. 75% of the fundamental output of the laser was introduced into TOPAS, which has optical frequency mixers resulting in tunable range from 285–1660 nm, while the rest of the output was used for white light generation. Typically, 2500 excitation pulses were averaged for 5 s to obtain the transient spectrum at a set delay time. Kinetic traces at appropriate wavelengths were assembled from the time-resolved spectral data. All measurements were conducted at 295 K.

Acknowledgements

Support by the National Science Foundation (Grant No. CHE-1110942 to F.D.), Grant-in-Aid (No. 20108010 to S.F. and 23750014 to K.O.), and the Global COE (center of excellence) program of Osaka University from MEXT, Japan (WCU R31-2008-000-10010-0), and NRF/MEST, Korea (GRL 2010-00353) programs is acknowledged.

[1] a) N. S. Lewis, D. G. Nocera, *Proc. Natl. Acad. Sci. USA* **2006**, *103*, 15729; b) P. V. Kamat, *J. Phys. Chem. C* **2007**, *111*, 2834; c) S. Fukuzumi, *Eur. J. Inorg. Chem.* **2008**, 1351.

[2] a) *Energy Harvesting Materials* (Ed.: D. L. Andrews), World Scientific, Singapore. **2005**; b) S. Günes, H. Neugebauer, N. S. Sariciftci, *Chem. Rev.* **2007**, *107*, 1324; c) H. Imahori, T. Umeyama, S. Ito, *Acc. Chem. Res.* **2009**, *42*, 1809; d) N. Armaroli, V. Balzani, *Angew. Chem.* **2007**, *119*, 52; *Angew. Chem. Int. Ed.* **2007**, *46*, 52.

[3] a) J. Deisenhofer, O. Epp, K. Miki, R. Huber, H. Michel, *J. Mol. Biol.* **1984**, *180*, 385; b) *The Photosynthetic Reaction Center* (Eds.: J. Deisenhofer, J. R. Norris), Academic Press, San Diego, CA. **1993**; c) C. Kirmaier, D. Holton in *The Photosynthetic Reaction Center, Vol II* (Eds.: J. Deisenhofer, J. R. Norris), Academic Press, San Diego, CA, **1993**, pp. 49–70.

[4] a) D. Gust, T. A. Moore, A. L. Moore, *Faraday Discuss.* **2012**, *155*, 9; b) S. D. Straight, G. Kodis, Y. Terazono, M. Hambourger, T. A. Moore, A. L. Moore, D. Gust, *Nat. Nanotechnol.* **2008**, *3*, 280; c) D. Gust, T. A. Moore, A. L. Moore, *Acc. Chem. Res.* **2001**, *34*, 40; d) D. Gust, T. A. Moore, A. L. Moore, *Acc. Chem. Res.* **2009**, *42*, 1890; e) D. Gust, T. A. Moore in *The Porphyrin Handbook, Vol. 8* (Eds.: K. M. Kadish, K. M. Smith, R. Guilard), Academic Press, Burlington, MA, **2000**, pp. 153–190.

[5] a) M. R. Wasielewski, *Chem. Rev.* **1992**, *92*, 435; b) R. F. Kelley, W. S. Shin, B. Rybtchinski, L. E. Sinks, M. R. Wasielewski, *J. Am. Chem. Soc.* **2007**, *129*, 3173; c) M. R. Wasielewski, *Acc. Chem. Res.* **2009**, *42*, 1910; d) V. L. Gunderson, S. M. Conron, M. R. Wasielewski, *Chem. Commun.* **2010**, *46*, 401; e) M. T. Vagnini, A. L. Smeigh, J. D. Blakemore, S. W. Eaton, N. D. Schley, F. D'Souza, R. H. Carbtree, G. W. Brudvig, D. T. Co, M. R. Wasielewski, *Proc. Natl. Acad. Sci. USA* **2012**, *109*, 15651.

[6] a) D. M. Guldi, *Chem. Commun.* **2011**, *47*, 606; b) D. M. Guldi, A. Rahman, V. Sgobba, C. Ehli, *Chem. Soc. Rev.* **2006**, *35*, 471; c) G. Bottari, G. de La Torre, D. M. Guldi, T. Torres, *Chem. Rev.* **2010**, *110*, 6768; d) N. Martín, L. Sanchez, M. A. Herranz, B. Illesca, D. M. Guldi, *Acc. Chem. Res.* **2007**, *40*, 1015; e) J. N. Clifford, G. Accorsi, F. Cardinali, J. F. Nierengarten, N. Armaroli, *C. R. Chemie* **2006**, *9*, 1005; f) J. L. Sessler, C. M. Lawrence, J. Jayawickramarajah, *Chem. Soc. Rev.* **2007**, *36*, 314; g) E. M. Pérez, N. Martín, *Chem. Soc. Rev.* **2008**, *37*, 1512.

[7] a) S. Fukuzumi, *Org. Biomol. Chem.* **2003**, *1*, 609; b) S. Fukuzumi, *Bull. Chem. Soc. Jpn.* **2006**, *79*, 177; c) S. Fukuzumi, *Phys. Chem. Chem. Phys.* **2008**, *10*, 2283; d) S. Fukuzumi, T. Kojima, *J. Mater. Chem.* **2008**, *18*, 1427; e) H. Imahori, S. Fukuzumi, *Adv. Funct. Mater.* **2004**, *14*, 525; f) S. Fukuzumi, *Pure Appl. Chem.* **2007**, *79*, 981; g) S. Fukuzumi, in *Functional Organic Materials* (Eds.: T. J. J. Müller U. H. F. Bunz), Wiley-VCH, Weinheim, **2007**, pp. 465–510; h) S. Fukuzumi, K. Ohkubo, *J. Mater. Chem.* **2012**, *22*, 4575; i) S. Fukuzumi, K. Ohkubo, F. D'Souza, J. L. Sessler, *Chem. Commun.* **2012**, *48*, 9801.

[8] a) S. Fukuzumi, K. Saito, K. Ohkubo, T. Khoury, Y. Kashiwagi, M. A. Absalom, S. Gadde, F. D'Souza, Y. Araki, O. Ito, M. J. Crossley, *Chem. Commun.* **2011**, *47*, 7980; b) T. Kojima, T. Honda, K. Ohkubo, M. Shiro, T. Kusukawa, T. Fukuda, N. Kobayashi, S. Fukuzumi, *Angew. Chem.* **2008**, *120*, 6814; *Angew. Chem. Int. Ed.* **2008**, *47*, 6712; c) J. L. Sessler, E. Karnas, S. K. Kim, Z. Ou, M. Zhang, K. M. Kadish, K. Ohkubo, S. Fukuzumi, *J. Am. Chem. Soc.* **2008**, *130*, 15256; d) S. Fukuzumi, K. Saito, K. Ohkubo, V. Troiani, H. Qui, S. Gadde, F. D'Souza, N. Solladié, *Phys. Chem. Chem. Phys.* **2011**, *13*, 17019; e) S. Fukuzumi, I. Amasaki, K. Ohkubo, C. P. Gros, R. Guilard, J.-M. Barbe, *RSC Adv.* **2012**, *2*, 3741; f) M. Tanaka, K. Ohkubo, C. P. Gross, R. Guilard, S. Fukuzumi, *J. Am. Chem. Soc.* **2006**, *128*, 14625; g) K. Ohkubo, Y. Kawashima, S. Fukuzumi, *Chem. Commun.* **2012**, *48*, 4314.

[9] a) F. D'Souza, O. Ito, *Chem. Commun.* **2009**, 4913; b) F. D'Souza, O. Ito, *Chem. Soc. Rev.* **2012**, *41*, 86; c) F. D'Souza, O. Ito, *Coord. Chem. Rev.* **2005**, *249*, 1410; d) M. E. El-Khouly, O. Ito, P. M. Smith, F. D'Souza, *J. Photochem. Photobiol. C* **2004**, *5*, 79; e) R. Chitta, F. D'Souza, *J. Mater. Chem.* **2008**, *18*, 1440; f) O. Ito, F. D'Souza, *Molecules* **2012**, *17*, 5816.

[10] a) *Introduction of Molecular Electronics* (Eds.: M. C. Petty, M. R. Bryce, D. Bloor), Oxford University Press, New York, **1995**; b) *Molecular Switches* (Ed.: B. L. Feringa), Wiley-VCH, Weinheim, **2001**.

[11] a) J. Killoran, L. Allen, J. F. Gallagher, W. M. Gallagher, D. F. O'Shea, *Chem. Commun.* **2002**, 1862; b) A. Gorman, J. Killoran, C. O'Shea, T. Kenna, W. M. Gallagher, D. F. O'Shea, *J. Am. Chem. Soc.* **2004**, *126*, 10619; c) K. Flavin, K. Lawrence, J. Bartelmess, M. Tasior, C. Navio, C. Bittencourt, D. F. O'Shea, D. M. Guldi, S. Giordani, *ACS Nano* **2011**, *5*, 1198.

[12] a) A. Loudet, K. Burgess, *Chem. Rev.* **2007**, *107*, 4891; b) G. Ulrich, R. Ziessel, A. Harriman, *Angew. Chem.* **2008**, *120*, 1202; *Angew. Chem. Int. Ed.* **2008**, *47*, 1184.

[13] a) M. J. Hall, S. O. McDonnell, J. Killoran, D. F. O'Shea, *J. Org. Chem.* **2005**, *70*, 5571; b) M. Tasior, D. F. O'Shea, *Bioconjugate Chem.* **2010**, *21*, 1130.

[14] A. N. Amin, M. E. El-Khouly, N. K. Subbaiyan, M. E. Zandler, M. Supur, S. Fukuzumi, F. D'Souza, *J. Phys. Chem. A* **2011**, *115*, 9810.

[15] A. N. Amin, M. E. El-Khouly, N. K. Subbaiyan, M. E. Zandler, S. Fukuzumi, F. D'Souza, *Chem. Commun.* **2012**, *48*, 206.

[16] a) M. E. El-Khouly, A. N. Amin, N. K. Subbaiyan, M. E. Zandler, S. Fukuzumi, F. D'Souza, *Chem. Eur. J.* **2012**, *18*, 5239; b) Y. Kataoka, Y. Shibata, H. Tamiaki, *Chem. Lett.* **2010**, *39*, 953.

[17] a) F. D'Souza, A. N. Amin, M. E. El-Khouly, N. K. Subbaiyan, M. E. Zandler, S. Fukuzumi, *J. Am. Chem. Soc.* **2012**, *134*, 654; b) V. Bandi, K. Ohkubo, S. Fukuzumi, F. D'Souza, *Chem. Commun.* **2013**, *49*, 2867; c) V. Bandi, M. E. El-Khouly, V. N. Nesterov, P. A. Karr, S. Fukuzumi, F. D'Souza, *J. Phys. Chem. C* **2013**, *117*, 5638.

[18] CCDC-908248 ((3,5-diphenyl-1*H*-pyrrol-2-yl)(3,5-diphenylpyrrol-2-ylidene)amine) contains the supplementary crystallographic data for this paper. These data can be obtained free of charge from The Cambridge Crystallographic Data Centre via www.ccdc.cam.ac.uk/data_request/cif. Crystal data for (3,5-diphenyl-1*H*-pyrrol-2-yl)(3,5-diphenylpyrrol-2-ylidene)amine: $C_{32}H_{23}N_3$; $M_w = 449.53\ g\,mol^{-1}$; $T = 100(2)$ K.; triclinic; space group $P\bar{1}$; unit cell dimensions: $a = 9.5414(8)$, $b = 10.1534(9)$, $c = 13.3161(17)$ Å; $\alpha = 100.761(1)$, $\beta = 100.175(1)$, $\gamma = 111.223(1)°$; $V = 1138.6(2)$ Å^3; $Z = 2$; $\rho_{calcd} = 1.311\ Mg\,m^{-3}$; absorption coefficient: $0.077\ mm^{-1}$; $F(000) = 472$; crystal size: $0.32 \times 0.12 \times 0.06\ mm^3$; theta range for data collection: 1.62–26.99°; reflections collected = 13641; independent reflections = 4945 [$R_{int} = 0.0218$]; absorption correction: semiempirical from equivalents; $R_1 = 0.0370$ [$I > 2\sigma(I)$]; $R_w = 0.0935$ (all data); GOF = 1.009.

[19] CCDC-908247 (**2b**) contains the supplementary crystallographic data for this paper. These data can be obtained free of charge from The Cambridge Crystallographic Data Centre via www.ccdc.cam.ac.uk/data_request/cif. Crystal data for **2b**: $C_{32}H_{22}BF_2N_3O_2$; $M_w = 529.34\ g\,mol^{-1}$; $T = 200(2)$ K.; orthorhombic; space group $Pca2_1$; unit cell dimensions: $a = 11.2390(19)$, $b = 12.232(2)$, $c = 36.786(6)$ Å; $\alpha = \beta = \gamma = 90°$; $V = 5057.4(14)$ Å^3; $Z = 8$; $\rho_{calcd} = 1.390\ Mg\,m^{-3}$; absorption coefficient: $0.097\ mm^{-1}$; $F(000) = 2192$; crystal size: $0.14 \times 0.05 \times 0.04\ mm^3$; theta range for data collection: 2.00–25.35°; reflections collected = 38344; independent reflections = 4700 [$R_{int} = 0.1122$]; absorption correction: semiempirical from equivalents; $R_1 = 0.0589$ [$I > 2\sigma(I)$]; $R_w = 0.1324$ (all data); GOF = 1.006.

[20] *Principles of Fluorescence Spectroscopy* (Ed.: J. R. Lakowicz), Springer, Singapore, **2006**.

[21] Gaussian 09, Revision B.01, M. J. Frisch, G. W. Trucks, H. B. Schlegel, G. E. Scuseria, M. A. Robb, J. R. Cheeseman, G. Scalmani, V. Barone, B. Mennucci, G. A. Petersson, H. Nakatsuji, M. Caricato, X. Li, H. P. Hratchian, A. F. Izmaylov, J. Bloino, G. Zheng, J. L. Sonnenberg, M. Hada, M. Ehara, K. Toyota, R. Fukuda, J. Hasegawa, M. Ishida, T. Nakajima, Y. Honda, O. Kitao, H. Nakai, T. Vreven, J. A. Montgomery, Jr, J. E. Peralta, F. Ogliaro, M. Bearpark, J. J. Heyd, E. Brothers, K. N. Kudin, V. N. Staroverov, T. Keith, R. Kobayashi, J. Normand, K. Raghavachari, A. Rendell, J. C. Burant, S. S. Iyengar, J. Tomasi, M. Cossi, N. Rega, J. M. Millam, M. Klene, J. E. Knox, J. B. Cross, V. Bakken, C. Adamo, J. Jaramillo, R. Gomperts, R. E. Stratmann, O. Yazyev, A. J. Austin, R. Cammi, C. Po-

melli, J. W. Ochterski, R. L. Martin, K. Morokuma, V. G. Zakrzewski, G. A. Voth, P. Salvador, J. J. Dannenberg, S. Dapprich, A. D. Daniels, O. Farkas, J. B. Foresman, J. V. Ortiz, J. Cioslowski and D. J. Fox, Gaussian, Inc, Wallingford CT, **2010**.

[22] For a general review on DFT applications of donor–acceptor systems see: M. E. Zandler, F. D'Souza, *C. R. Chemie* **2006**, *9*, 960.

[23] N. Mataga, H. Miyasaka, in *Electron Transfer* (Eds.: J. Jortner, M. Bixon), Wiley, New York. **1999**, Part 2, pp. 431–496.

[24] $\Delta G_{CR} = e(E_{ox} - E_{red})$; $-\Delta G_{CS} = \Delta E_{00} - (-\Delta G_{CR})$, in which ΔE_{00} is the energy of ^{1}ADP* and $^1C_{60}$*. The electrostatic energy was neglected in a polar solvent (PhCN).

[25] a) R. A. Marcus, *Angew. Chem.* **1993**, *105*, 1161; *Angew. Chem. Int. Ed. Engl.* **1993**, *32*, 1111; b) R. A. Marcus, N. Sutin, *Biochim. Biophys. Acta.* **1985**, *811*, 265.

[26] Y. Araki, Y. Yasumura, O. Ito, *J. Phys. Chem. B* **2005**, *109*, 9843.

Received: December 4, 2012
Revised: February 23, 2013
Published online: March 28, 2013

